Mitochondrial Calcium Transients in Adult Rabbit Cardiac Myocytes: Inhibition by Ruthenium Red and Artifacts Caused by Lysosomal Loading of Ca^{2+}-Indicating Fluorophores

Donna R. Trollinger,* Wayne E. Cascio,† and John J. Lemasters*
Departments of *Cell Biology and Anatomy and †Medicine, School of Medicine, University of North Carolina, Chapel Hill, North Carolina 27599-7090 USA

ABSTRACT A cold/warm loading protocol was used to ester-load Rhod 2 into mitochondria and other organelles and Fluo 3 into the cytosol of adult rabbit cardiac myocytes for confocal fluorescence imaging. Transient increases in both cytosolic Fluo 3 and mitochondrial Rhod 2 fluorescence occurred after electrical stimulation. Ruthenium red, a blocker of the mitochondrial Ca^{2+} uniporter, inhibited mitochondrial Rhod 2 fluorescence transients but not cytosolic Fluo 3 transients. Thus the ruthenium red-sensitive mitochondrial Ca^{2+} uniporter catalyzes Ca^{2+} uptake during beat-to-beat transients of mitochondrial free Ca^{2+}, which in turn may help match mitochondrial ATP production to myocardial ATP demand. After ester loading, substantial amounts of Ca^{2+}-indicating fluorophores localized into an acidic lysosomal/endosomal compartment. This lysosomal fluorescence did not respond to electrical stimulation. Because fluorescence arose predominantly from lysosomes after the cold loading/warm incubation procedure, total cellular fluorescence failed to track beat-to-beat changes of mitochondrial fluorescence. Only three-dimensionally resolved confocal imaging distinguished the relatively weak mitochondrial signal from the bright lysosomal fluorescence.

INTRODUCTION

In the heart at maximum cardiac output, total ATP and creatine phosphate turn over every few seconds (Achterberg, 1988; Taegtmeyer, 1988). Because heart rate and cardiac output increase within seconds in response to exertion, ATP production by oxidative phosphorylation must respond on virtually a beat-to-beat basis to avoid large fluctuations of myocardial ATP and creatine phosphate in response to changes of cardiac output. One factor proposed to regulate mitochondrial metabolism is intramitochondrial Ca^{2+}, because pyruvate dehydrogenase, isocitrate dehydrogenase, and α-ketoglutarate dehydrogenase are each activated by submicromolar Ca^{2+} (McCormack and Denton, 1979; Williamson and Cooper, 1980; Hansford, 1981). Other evidence suggests that Ca^{2+} may also activate mitochondrial respiration, adenine nucleotide translocation, and ATP synthetase activity (Moreno-Sanchez, 1985a,b; Halestrap, 1987).

A controversial issue is whether changes in mitochondrial Ca^{2+} are kinetically competent to regulate mitochondrial ATP formation in response to rapid changes in myocardial work. Elemental microanalysis of rapidly frozen cardiac myocytes revealed a fourfold increase in total mitochondrial Ca^{2+} 50 ms after electrical stimulation (Wendt-Gallitelli and Isenberg, 1991; Isenberg et al., 1993; Gallitelli et al., 1999; but see Moravec and Bond, 1991). In contrast, microfluorometry of Ca^{2+}-indicating fluorophores in noncytosolic (presumably mitochondrial) compartments of single cardiac myocytes showed a slow increase in mitochondrial Ca^{2+} over tens of seconds in response to increased electrical pacing, but no rapid mitochondrial Ca^{2+} transients with each single contraction (Miyata et al., 1991; Di Lisa et al., 1993; Griffiths et al., 1997). The same techniques were used to measure changes in mitochondrial Ca^{2+} during ischemia/hypoxia and reoxygenation (Miyata et al., 1992; Griffiths et al., 1998). However, we recently applied confocal microscopy to measure mitochondrial free Ca^{2+} in adult rabbit cardiac myocytes and observed rapid beat-to-beat mitochondrial transients during electrical pacing (Chacon et al., 1996; Trollinger et al., 1997; Ohata et al., 1998).

The apparent K_m for uptake of Ca^{2+} through the ruthenium red-sensitive uniporter in isolated mitochondria is several times the levels of cytosolic free Ca^{2+} in myocytes (Gunter and Pfeiffer, 1990). Modeling of the kinetic characteristics of Ca^{2+} uptake and release by isolated mitochondria leads to the conclusion that mitochondria are unable to take up and release significant amounts of Ca^{2+} during the contractile cycle (Nicholls and Crompton, 1980). However, the kinetic characteristics of enzymes and transporters in situ within living cells may be quite different from what is measured in vitro. In particular, polyamines such as spermine, which exist at millimolar concentrations in the cytosol, decrease the K_m of Ca^{2+} uptake by isolated mitochondria (Nicchitta and Williamson, 1984).

Accordingly, the goal of the present study was to determine whether the rapid mitochondrial Ca^{2+} uptake observed by confocal microscopy during the contractile cycle involves the ruthenium red-sensitive mitochondrial Ca^{2+}

Received for publication 3 June 1999 and in final form 19 March 2000.

Address reprint requests to Dr. John J. Lemasters, Department of Cell Biology, University of North Carolina at Chapel Hill, CB 7090, 236 Taylor Hall, Chapel Hill, NC 27599-7090. Tel.: 919-966-5507; Fax: 919-966-7197; E-mail: lemaster@med.unc.edu.

Dr. Trollinger's present address is Department of Molecular and Cell Biology, University of California, Davis, One Shields Avenue, Davis, CA 95616.

0006-3495/00/07/39/12 $2.00

uniporter. Furthermore, we sought to better characterize the noncytosolic uptake of ester-loaded Ca^{2+}-indicating fluorophores. Our results show that ruthenium red specifically inhibits mitochondrial but not cytosolic Ca^{2+} transients during the contractile cycle. Moreover, we show substantial uptake of Ca^{2+}-indicating fluorophores into the lysosomal/endosomal compartment after ester loading. This lysosomal loading obscures the observation of mitochondrial Ca^{2+} transients by whole-cell fluorescence measurements.

EXPERIMENTAL PROCEDURES

Myocyte isolation

Adult cardiac myocytes were isolated from New Zealand white rabbits (3–4 kg) by collagenase/hyaluronidase digestion, as previously described (Trollinger et al., 1997), and attached to laminin-coated coverslips (10 $\mu g/cm^2$) for 2 h in an air/5% CO_2 incubator at 37°C in nutrient medium (1:1 mixture of Joklik's medium and medium 199 supplemented with 0.05 U/ml insulin, 1 mM creatine, 1 mM octanoic acid, 1 mM taurine, 10 U/ml penicillin, and 10 mg/ml streptomycin). All experiments were performed within 12 h of plating and at room temperature in Krebs-Ringer-HEPES buffer (KRH) (110 mM NaCl, 5.0 mM KCl, 1.25 mM $CaCl_2$, 0.5 mM Na_2HPO_4, 0.5 mM KH_2PO_4, 1.0 mM $MgSO_4$, 10 mM glucose, 1.0 mM octanoic acid, and 20 mM HEPES) containing 1 μM isoproterenol at pH 7.4.

Two-step cold loading/warm incubation protocol

Myocytes were loaded with Rhod 2-AM (5 μM) for 30 min at 4°C or Fluo 3-AM (10 μM) for 30 min at 4°C in HEPES-buffered nutrient medium (20 mM HEPES) containing 10% fetal calf serum at pH 7.4. After cold loading, cells were incubated for 4–6 h at 37°C in nutrient medium without serum. Before mounting on the microscope, cells were washed twice with KRH.

Warm loading of fluorophores

Myocytes were loaded with Fluo 3-AM (10 μM), LysoTracker red (50 nM), and/or Rhodamine 123 (1 μM) at 37°C for 15–30 min in nutrient medium without serum.

Electrical simulation

Myocytes were field depolarized at twice the threshold voltage in 5-ms pulses with a Grass model SD9 stimulator (Quincy, MA).

Confocal fluorescence imaging

Images of green fluorescence (Fluo 3, Rhodamine 123) and red fluorescence (Rhod 2, LysoTracker Red) were collected at 23°C with a Zeiss 410 laser scanning confocal microscope. Pinhole settings were set to maximize optical sectioning, which was ~0.9 μm. Green and red fluorescence were excited, respectively, with the 488- and 568-nm lines of an argon-krypton laser. Red and green fluorescence were directed to separate photomultipliers by a 560-nm long-pass dichroic reflector through 590-nm long-pass and 522-nm (35-nm bandpass) barrier filters, respectively. Images were pseudocolored using the black body look-up table of Photoshop (Adobe Systems, San Jose, CA), as shown by insets in the figures. Plot analyses were performed using Image PC (Scion Corp., Frederick, MD).

Materials

Br-A23187 and ruthenium red were obtained from Sigma (St. Louis, MO). Rhod 2-AM, Fluo 3-AM, Rhodamine 123, and LysoTracker Red were obtained from Molecular Probes (Eugene, OR). All other reagents were of analytical grade and were obtained from the usual commercial sources.

RESULTS

Inhibition by ruthenium red of mitochondrial Ca^{2+} transients during the contractile cycle

Ca^{2+}-tolerant adult rabbit cardiac myocytes were isolated by enzymatic digestion and plated on glass coverslips (see Experimental Procedures). Myocytes were then subjected to a two-step loading protocol (Trollinger et al., 1997). Initially, myocytes were incubated with Rhod 2-AM for 30 min at 4°C. Such cold loading localized Rhod 2 to both cytosolic and noncytosolic organellar compartments, including mitochondria. Subsequently, the myocytes were incubated at 37°C for 4–6 h. This second step permitted leakage of cytosolic Rhod 2 with retention of Rhod 2 trapped in mitochondria and other organelles. Confocal images of myocytes loaded with Rhod 2 in this fashion revealed a characteristic mitochondrial pattern (Fig. 1 *a*; compare with Fig. 7 *a*). The myocyte in Fig. 1 *a* was then electrically stimulated during the collection of a 16-s confocal scan. Rhod 2 fluorescence rapidly increased and decreased after each stimulation, producing horizontal banding in the image as the scan proceeded from top to bottom (Fig. 1 *b*). To quantify the transients of Rhod 2 fluorescence, the average intensity of each row of pixels in the *x* direction was plotted against scan time in the *y* direction for the selected area outlined by white lines. This plot analysis showed that fluorescence increased by an average of 93% after each stimulation (Fig. 2).

Ruthenium red inhibits mitochondrial Ca^{2+} uniport (Moore, 1971; Reed and Bygrave, 1974) but crosses the plasma membrane of intact cells slowly (see Matlib et al., 1998). Thus little change in mitochondrial Ca^{2+} transients was observed in the first few minutes after the addition of 10 μM ruthenium red (not shown). After 20 min, however, mitochondrial Ca^{2+} transients were suppressed (Fig. 1 *c*), although the cells continued to contract. Plot analysis confirmed the inhibition of the Rhod 2 fluorescence transients by ruthenium red (Fig. 2, *middle*). In the right panel of Fig. 2, we plotted the average of five consecutive fluorescence transients before and after ruthenium red addition. The initial rate of rise of Rhod 2 fluorescence after electrical stimulation was inhibited by 85% by ruthenium red, whereas the peak fluorescence change in the averaged transients was suppressed by 58%. Similar results were obtained in two other independent experiments.

The residual Rhod 2 fluorescence transient after ruthenium red may represent either the cytosolic Ca^{2+} transient due to retention of some Rhod 2 in the cytosol or to an

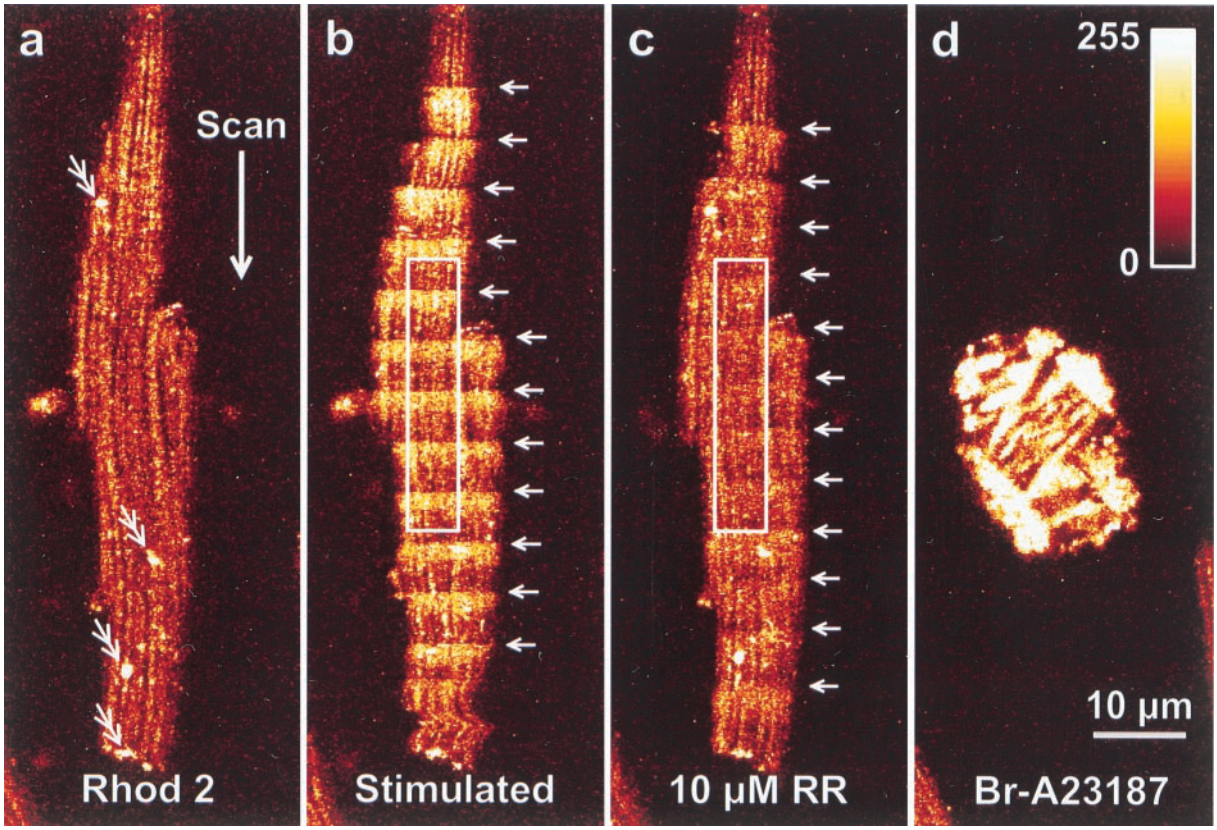

FIGURE 1 Inhibition by ruthenium red of mitochondrial Ca^{2+} transients after electrical stimulation. A cardiac myocyte was loaded with Rhod 2-AM (5 μM) at 4°C for 30 min followed by warm incubation at 37°C for 5 h. Sixteen-second confocal scans of red Rhod 2 fluorescence were then collected, which progressed from top to bottom in each image. (*a*) Confocal imaging of Rhod 2 fluorescence after cold loading/warm incubation showed a mitochondrial pattern of labeling. Double arrows label bright spots of lysosomal fluorescence (see Fig. 6). (*b*) The myocyte was stimulated at 1 Hz. Rhod 2 fluorescence increased and decreased in the mitochondria to produce horizontal banding in the 16-s scans (*arrows*). (*c*) Ruthenium red (RR) (10 μM) was added, and another confocal image was collected after 20 min. In the presence of ruthenium red, mitochondrial Ca^{2+} transients were suppressed. (*d*) Oligomycin (10 μM), CCCP (10 μM), and then Br-A23187 (20 μM) were added at the end of the experiment to increase Ca^{2+} everywhere inside the cell and saturate Rhod 2 fluorescence. Under these conditions, Rhod 2 was confined almost exclusively to mitochondria. This is one experiment that is representative of three.

incomplete inhibition of the mitochondrial Ca^{2+} transient by the poorly penetrating ruthenium red. Previously we showed that cytosolic Ca^{2+} transients are no slower than the observed mitochondrial transients (Chacon et al., 1996; Ohata et al., 1998). Because Rhod 2 fluorescence transients became considerably slower in the presence of ruthenium red and plateaued after ~190 ms rather than after 60 ms (Fig. 2), the residual Rhod 2 fluorescence transient after ruthenium red inhibition likely represents an attenuated mitochondrial transient.

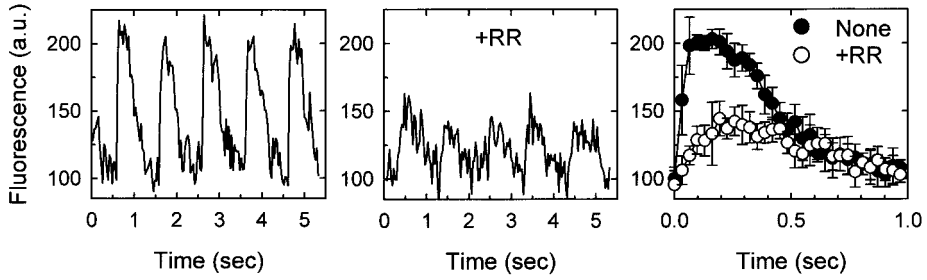

FIGURE 2 Plot analysis of mitochondrial Ca^{2+} transients before and after ruthenium red. In the left and middle panels, the average intensity for each row of pixels in the *x* direction in arbitrary units (a.u.) was plotted against scan time calculated from the *y* axis position. Selected areas with few bright lysosomal spots (see Fig. 6) were used, as outlined in white in Fig. 1, *b* and *c*. In the right-hand panel, fluorescent transients during five consecutive stimulations were averaged in the absence (●) and presence (○) of ruthenium red from the selected areas shown in Fig. 1, *b* and *c*. Error bars are SD.

Subsequently Br-A23187, a Ca^{2+} ionophore, was added to saturate Rhod 2 in all compartments and reveal the intracellular distribution of the fluorophore. In addition, an uncoupler, carbonylcyanide m-chlorophenylhydrazone (CCCP), was added to depolarize the mitochondrial inner membrane and prevent electrophoretic uptake of Ca^{2+} into the mitochondrial space in excess of cytosolic Ca^{2+} concentration. Oligomycin was also added to prevent ATP depletion by the uncoupler-stimulated mitochondrial ATPase and subsequent cell death (Nieminen et al., 1990, 1994). Increased intracellular Ca^{2+} after the addition of Br-A23187, CCCP, and oligomycin led to contracture (Fig. 1 *d*), but Rhod 2 fluorescence remained confined to mitochondria, which were distorted into round and oblong masses by the contracture. Contracture demonstrated that cytosolic Ca^{2+} was indeed elevated. Nonetheless, cytosolic spaces between mitochondria remained dark. Previously we prevented contracture by using butanedione monoxime. In the absence of contracture, Br-A23187 produced a pattern of Rhod 2 fluorescence after the cold loading/warm incubation protocol that was identical to the pattern observed in normal cells labeled with the mitochondrial markers rhodamine 123 and tetramethylrhodamine methylester (Trollinger et al., 1997).

Lack of inhibition by ruthenium red of cytosolic Ca^{2+} transients during the contractile cycle

Ruthenium red compounds are reported to inhibit Ca^{2+} release from the ryanodine channels of the sarcoplasmic reticulum (Chamberlain et al., 1984; Chiesi et al., 1988; Calviello and Chiesi, 1989). Although the ryanodine channel of cardiac muscle is less sensitive to ruthenium red inhibition than skeletal muscle, we wanted to exclude the possibility that the ruthenium red blockade of mitochondrial Ca^{2+} transients was secondary to suppression of cytosolic Ca^{2+} transients. Accordingly, myocytes were loaded with 10 μM Fluo 3-AM at 37°C. Warm loading under these conditions favors cytosolic over mitochondrial loading (Nieminen et al., 1995; Trollinger et al., 1997; Ohata et al., 1998). In unstimulated cells, Fluo 3 fluorescence was dim and diffuse (Fig. 3 *a*), except for a few bright spots (*double arrows*) that corresponded to acidic lysosomes (see below), which were also observed after cold ester loading of Rhod 2 (Fig. 1 *a*, *double arrows*). Faint striations were also present, which may represent some Fluo 3 uptake into the sarcoplasmic reticulum, as reported for endoplasmic and sarcoplasmic reticulum (Golovina and Blaustein, 1997). When Fluo 3-loaded myocytes were electrically stimulated, fluorescence increased after

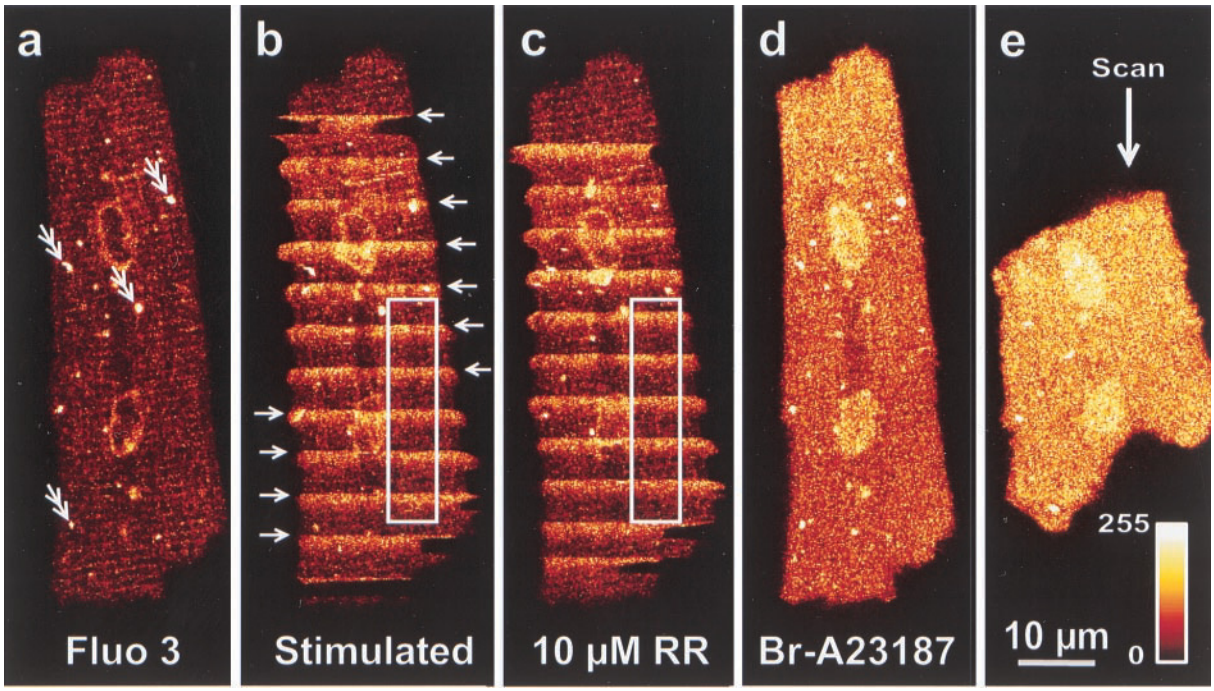

FIGURE 3 Lack of inhibition by ruthenium red of cytosolic Ca^{2+} transients after electrical stimulation. A cardiac myocyte was loaded with Fluo 3-AM (10 μM) at 37°C for 15 min before confocal imaging. (*a*) Note that Fluo 3 fluorescence was diffuse throughout the cell, except for occasional bright lysosomal spots (*double arrows*; see Fig. 6) and some faint striations, the latter possibly due to a small amount of Fluo 3 uptake into the sarcoplasmic reticulum. (*b*) During electrical stimulation at 1 Hz, Fluo 3 fluorescence increased and decreased to produce horizontal banding in the 16-s scan. (*c*) The subsequent addition of 10 μM ruthenium red (RR) as in Fig. 1 did not block these cytosolic fluorescence transients. (*d*) After the addition of oligomycin, CCCP, and Br-A23187 as described in Fig. 1, Fluo 3 fluorescence rose throughout the cytoplasm, which demonstrated cytosolic loading of fluorophore. (*e*) After 15 min of exposure to Br-A23187, the myocyte shortened. This is one experiment that is representative of three.

each stimulation, again producing horizontal banding as the scan progressed from top to bottom (Fig. 3 *b*). Plot analysis revealed that Fluo 3 fluorescence increased by an average of 196% after each stimulation (Fig. 4).

Subsequently, ruthenium red was added, and images were collected after 20 min. In contrast to myocytes loaded with Rhod 2 by the two-step cold loading/warm incubation protocol, ruthenium red treatment did not suppress cytosolic Ca^{2+} transients of Fluo 3-loaded myocytes (Fig. 3 *c*). Plot analyses confirmed the lack of inhibition of Fluo 3 fluorescence transients by ruthenium red (compare *left* and *middle panels* of Fig. 4). Indeed, averaged fluorescence transients before and after ruthenium red addition were virtually indistinguishable (Fig. 4, *right*). When Br-A23187 was then added, Fluo 3 fluorescence increased diffusely throughout the myocyte (Fig. 3, *d* and *e*). Under ideal imaging conditions, mitochondria can be imaged as dark voids within a fluorescently labeled cytosol (Nieminen et al., 1995; Chacon et al., 1996; Ohata et al., 1998). In the present experiments, however, we restricted our excitation energy to minimize photodamage. Thus negative imaging of mitochondria was limited by spatial signal-to-noise, although some negative imaging of a cluster of perinuclear mitochondria was evident between the two nuclei of the binucleate myocyte. Similar results were obtained in two other experiments.

Mitochondrial and cytosolic Ca^{2+} transients in a myocyte loaded simultaneously with Rhod 2 in mitochondria and Fluo 3 in the cytosol

To exclude the possibility that ruthenium red was acting differently in the different experiments, we again labeled myocytes with Rhod 2 by a cold loading/warm incubation protocol. After the warm incubation, we loaded cells with 10 μM Fluo 3-AM for 15 min at 37°C. Our aim was to load Fluo 3 into the cytosol and Rhod 2 into the mitochondria. After this coloading procedure, red Rhod 2 fluorescence of unstimulated myocytes again showed a mitochondrial pattern (Fig. 5 *a*). Except for lysosomal uptake, green Fluo 3 fluorescence showed a diffuse cytosolic pattern (Fig. 5 *a′*). During stimulation, both Rhod 2 and Fluo 3 images showed horizontal banding indicative of Ca^{2+} transients (Fig. 5, *b* and *b′*). After the addition of ruthenium red, Rhod 2 fluorescence transients were suppressed after 20 min (Fig. 5 *c*), but the Fluo 3 transients remained prominent (Fig. 5 *c′*). Electrical stimulation in the experiment of Fig. 5 was close to threshold, and some electrical stimulations failed to cause any Ca^{2+} transients at all. This occurred both before and after the addition of ruthenium red. However, when electrical stimulation did produce a response, the individual cytosolic Ca^{2+} transients were as strong after the addition of ruthenium red as before, whereas the mitochondrial transients were strongly suppressed by ruthenium red.

Subsequently, low-Na^+ buffer was added to increase intracellular Ca^{2+} by reversal of the sarcolemmal Na^+/Ca^{2+} exchanger. In the Rhod 2 image, fluorescence increased in mitochondria but not in toxic blebs containing cytosol (Fig. 5 *d*, *double arrows*), whereas Fluo 3 fluorescence increased diffusely throughout the cytosol, including inside blebs (Fig. 5 *d′*). Together, Figs. 1–5 show that ruthenium red specifically blocks mitochondrial Ca^{2+} transients but not cytosolic Ca^{2+} transients during electrical pacing. Thus the ruthenium red-sensitive Ca^{2+} uniporter of the mitochondrial inner membrane mediates mitochondrial Ca^{2+} uptake during the contractile cycle.

Lysosomal localization of Ca^{2+}-indicating fluorophores after ester loading

As mentioned above, small bright spots of fluorescence were observed throughout the cytoplasm after both cold and warm ester loading of Ca^{2+}-indicating fluorophores (Figs. 1 *a* and 3 *a*, *double arrows*). Previously we suspected that these bright spots of fluorescence represented lysosomes (Trollinger et al., 1997; Ohata et al., 1998). To test this hypothesis, we loaded myocytes with green-fluorescing Fluo 3 by our cold loading/warm incubation protocol. We then incubated the cells with LysoTracker Red, a red-fluorescing fluorophore that localizes to the acidic lysosomal/

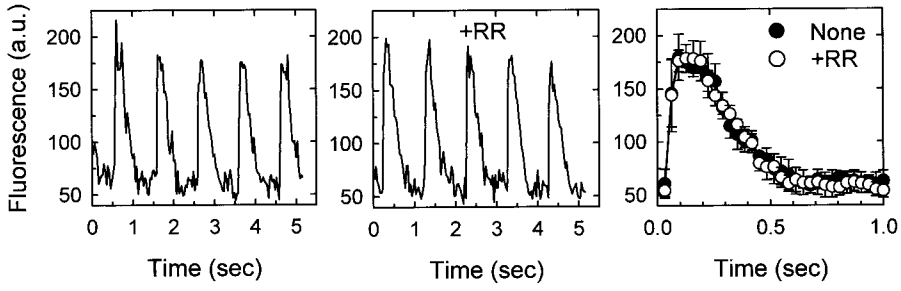

FIGURE 4 Plot analysis of cytosolic Ca^{2+} transients before and after ruthenium red. In the left and middle panels, the average *x* axis pixel fluorescence intensity was plotted versus time for the selected areas outlined in white in Fig. 3, *b* and *c*, as described in the legend to Fig. 2. In the right panel, fluorescent transients during five consecutive stimulations were averaged in the absence (●) and presence (○) of ruthenium red from the selected areas shown in Fig. 3, *b* and *c*. Error bars are SD.

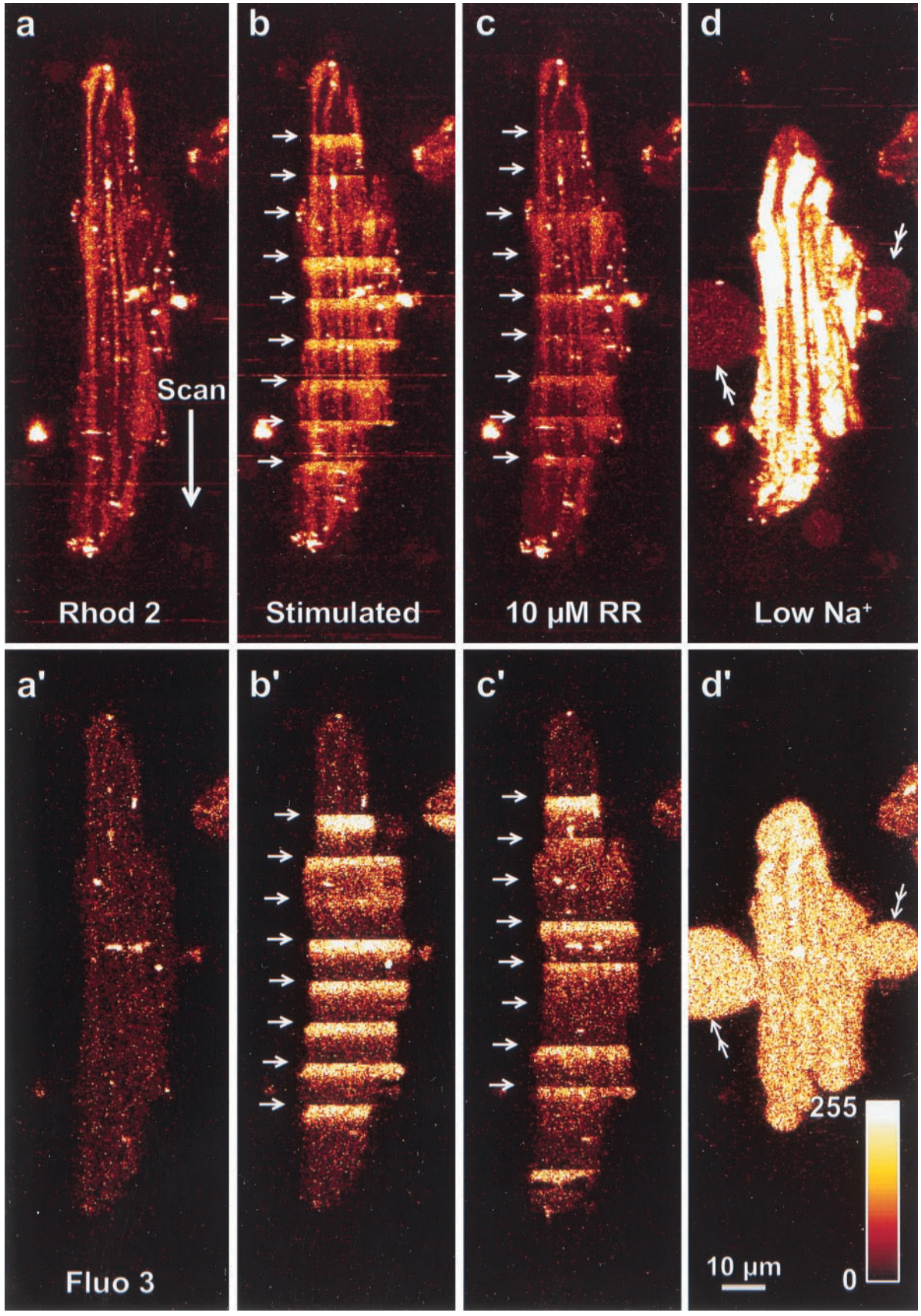
a
b
c
d
Scan
Rhod 2
Stimulated
10 μM RR
Low Na+
a'
b'
c'
d'
Fluo 3
255
0
10 μm

endosomal compartment. Confocal images of LysoTracker Red showed many small punctate structures that represent lysosomes and associated acidic endosomes (Fig. 6 *a*). An image of the green fluorescence of Fluo 3 was then obtained. Most Fluo 3 fluorescence colocalized to lysosomes labeled with LysoTracker Red (compare Fig. 6, *a* and *b*). Indeed, the majority of total Fluo 3 fluorescence was lysosomal. Selected area analysis showed a correlation coefficient (r) of 0.779 ($p < 0.0001$) for fluorescence intensity values between corresponding pixels in the Fluo 3 and LysoTracker Red images.

Although acidic lysosomal/endosomal compartments were dispersed throughout the cytoplasm, their disposition was not entirely random. When the image was aligned to the long axis of the myocyte (box in Fig. 6 *a*), the plot of average intensity of each row of pixels in the x direction against y axis position showed peaks with a periodicity of 1.9 μm (Fig. 6 *c*). Thus lysosomal position seems to be aligned with the sarcomeric repeat, although only a small proportion of all sarcomeres in individual myofibrils were associated with lysosomes.

Contribution of lysosomes and mitochondria to total cellular fluorescence after cold loading/ warm incubation of Rhod 2

The question now arises: How can mitochondrial Ca^{2+} be measured if most fluorescence arises from lysosomes? To address this issue, a myocyte was cold loaded with Rhod 2 followed by warm incubation, as described above. Then the cell was loaded with green-fluorescing Rhodamine 123, which was taken up by mitochondria. Rhodamine 123 fluorescence illustrated the typical distribution of mitochondria within a myocyte (Fig. 7 *a*). An image of the red fluorescence of Rhod 2 was then collected during electrical stimulation. Our confocal microscope can only record a linear scale of 256 gray levels (0–255), and intensity levels exceeding this range were recorded as a value of 255. Accordingly, we used laser illumination of low intensity, so that the brightest spots of fluorescence arising from lysosomes would not exceed an intensity value of 254 (Fig. 7 *b*). Images obtained in this way fairly represented the intracellular distribution of total Rhod 2 fluorescence arising from the myocyte. As can readily be seen, Rhod 2 fluorescence under these conditions bore little relation to the distribution of Rhodamine 123-labeled mitochondria (compare Fig. 7, *a* and *b*). Rather, the distribution of Rhod 2 fluorescence corresponded to the pattern of lysosomal fluorescence shown in Fig. 6 *a*. The image in Fig. 7 *b* was collected during electrical stimulation, but no fluorescence transients were observed at this low level of laser illumination. A plot of average intensity for each row of pixels in the x direction (an unbiased sampling of total cellular fluorescence) versus scan time in the y direction also did not show fluorescence transients (Fig. 8, *left*). Rather, the plot analysis showed random fluctuations of average x axis intensity as the scan in the y direction encountered individual lysosomes.

Next we repeated the confocal scan, using 100 times more laser excitation intensity. Fluorescence arising from lysosomes was now saturated and was recorded as gray-level intensities of 255 (Fig. 7 *c*). At this higher excitation, a mitochondrial pattern of fluorescence could now be identified in addition to the original lysosomal pattern of fluorescence. Moreover, this mitochondrial fluorescence showed transients during electrical stimulation, as revealed by the appearance of horizontal banding (Fig. 7 *d*). Similarly, at excitation 100 times greater, the plot analysis showed repetitive fluorescence transients with each electrical stimulation (Fig. 8, *right, arrows*), which were not present in the absence of stimulation (Fig. 8, *middle*). In contrast to the plot analyses shown in Figs. 2 and 4, which were performed in small selected areas containing few lysosomes, the plot analysis shown in Fig. 8 was performed over the entire myocyte. Consequently, in the absence of electrical stimulation, the average fluorescence for each row of pixels in the x direction fluctuated irregularly as the scan in the y direction encountered the highly fluorescent lysosomes (Fig. 8, *middle*). Subsequent electrical pacing then produced regularly repeating fluorescence transients that were superimposed on this irregular background (Fig. 8, *right*). Taken together, these experiments document that rapid Ca^{2+} transients occur in mitochondria that are readily observable by confocal imaging but not by total cellular fluorescence.

FIGURE 5 Ruthenium red inhibition of Ca^{2+} transients in myocytes coloaded with Rhod 2 and Fluo 3. Myocytes were labeled with Rhod 2-AM by the cold loading/warm incubation protocol described in Fig. 1. After warm incubation, the myocytes were then loaded with Fluo 3-AM (10 μM) for 15 min at 37°C. After washing with KRH, confocal images of red Rhod 2 fluorescence (>590 nm) excited by 568 nm light and green Fluo 3 fluorescence (505–540 nm) excited by 488 nm light were collected in sequential 16-s scans, as described in Fig. 1. (*a*) Before stimulation, Rhod 2 fluorescence showed a mitochondrial pattern. (*a′*) Fluo 3 fluorescence showed predominantly a diffuse pattern, except for small spots of lysosomal fluorescence (see Fig. 6). (*b* and *b′*) Both Rhod 2 and Fluo 3 fluorescence showed horizontal banding when confocal images were collected during electrical stimulation. This banding indicated mitochondrial and cytosolic Ca^{2+} transients, respectively (*b* and *b′*, *arrows*). (*c*) Rhod 2 fluorescence transients were suppressed 20 min after the addition of 10 μM ruthenium red (RR), but (*c′*) the Fluo 3 fluorescence transients remained. Electrical stimulation in this experiment was close to threshold, and some electrical stimulations failed to induce Ca^{2+} transients. This occurred both before and after the addition of ruthenium red. When electrical stimulation did produce a response, individual cytosolic Ca^{2+} transients were as strong after ruthenium red as before, whereas the mitochondrial transients were strongly suppressed. Subsequently, K^+-substituted, low-Na^+ KRH (5 mM Na^+) was added to increase intracellular Ca^{2+} by reverse Na^+/Ca^{2+} exchange (*d* and *d′*). (*d*) Rhod 2 fluorescence increased inside mitochondria, but not in toxic blebs (*double arrows*), whereas (*d′*) Fluo 3 fluorescence increased diffusely in both the cytosol and blebs (*double arrows*).

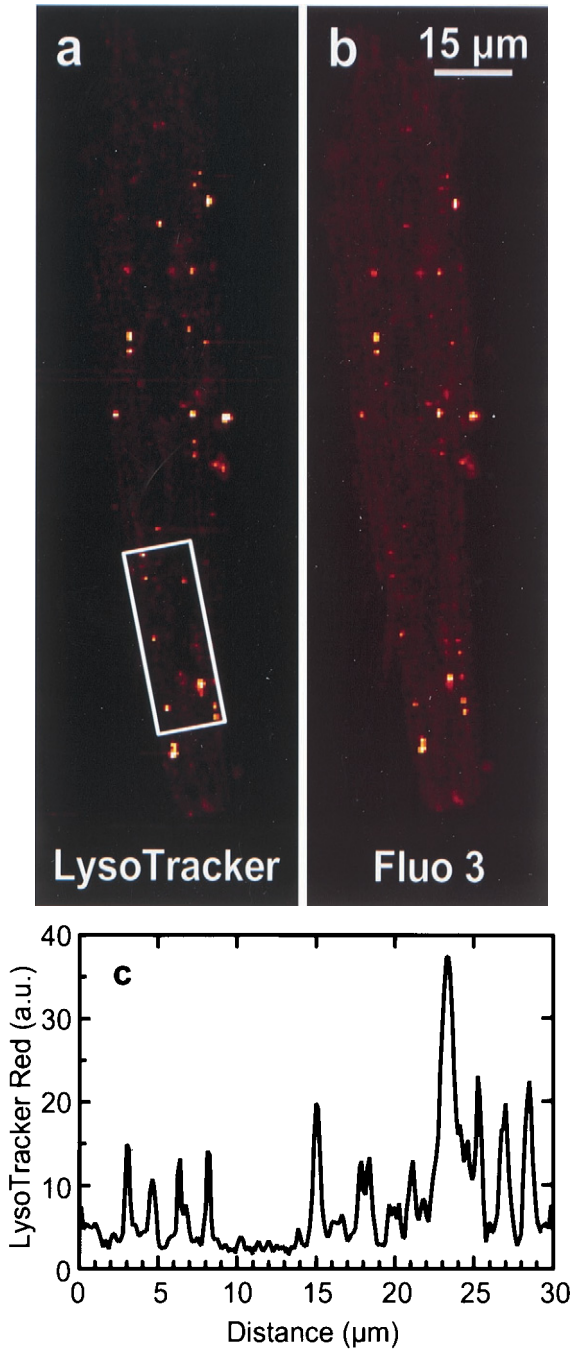

FIGURE 6 Lysosomal localization of Fluo 3 after ester loading. Myocytes were loaded with 10 μM Fluo 3-AM by the cold loading/warm incubation protocol, as described in Fig. 1 for Rhod 2, and then incubated with LysoTracker Red (50 nM) for 20 min at 37°C to label lysosomes. (*a*) Red LysoTracker Red fluorescence was imaged. (*b*) Green Fluo 3 fluorescence was imaged. LysoTracker Red and Fluo 3 colocalized in heterogeneous punctate structures that represent lysosomes and associated acidic endosomes. The Pearson correlation coefficient between intracellular pixel intensity values of the LysoTracker Red and Fluo 3 images was 0.779 ($p < 0.0001$). (*c*) A plot analysis of average *x* axis pixel intensity at each *y* axis position parallel to the myocyte long axis shows peaks of LysoTracker Red fluorescence at a periodicity of 1.9 μm. The white lines in *a* outline the selected area used in the plot analysis.

DISCUSSION

Inhibition of mitochondrial Ca^{2+} transients in cardiac myocytes by ruthenium red

Here we show for the first time that ruthenium red inhibits the rapid mitochondrial Ca^{2+} transients that accompany each contractile cycle in adult rabbit cardiac myocytes (Fig. 1). Ruthenium red produced a 58% decrease in the peak of the transient and a 85% decrease of the initial rate of rise of the transient (Fig. 2). Because ruthenium red permeates the sarcolemma slowly (Matlib et al., 1998), inhibition did not become evident until many minutes after the ruthenium red addition. Thus we routinely made our measurements 20 min after the addition of 10 μM ruthenium red.

Ruthenium red inhibits Ca^{2+} uptake by isolated heart mitochondria with an IC_{50} of 7 nM (Matlib et al., 1998). Ruthenium red also inhibits the Ca^{2+} release channel of isolated cardiac sarcoplasmic reticulum, but the IC_{50} is much greater (>2 μM) (Chiesi et al., 1988). In digitonin-permeabilized rat cardiac myocytes, the IC_{50} for the inhibition of Ca^{2+} release from the sarcoplasmic reticulum is 5–10 μM (Matlib et al., 1998). Although inhibition of Ca^{2+} release from the sarcoplasmic reticulum of nonpermeabilized myocytes will be even weaker because of the very slow permeation of ruthenium red, one mechanism of inhibition of mitochondrial Ca^{2+} transients could be an inhibition of cytosolic Ca^{2+} transients secondary to blockade of cytosolic Ca^{2+} influx from the sarcoplasmic reticulum. To exclude this possibility, we loaded Fluo 3 into the cytosol, and we observed that ruthenium red had virtually no effect on cytosolic Ca^{2+} transients during the contractile cycle (Figs. 3 and 4). To ensure that ruthenium red was actually penetrating the myocytes in these experiments, we developed a new technique to load one Ca^{2+} indicator into the mitochondria (Rhod 2) and a second indicator into the cytosol (Fluo 3). In myocytes coloaded in this fashion, ruthenium red inhibited mitochondrial transients of Rhod 2 fluorescence but not cytosolic transients of Fluo 3 fluorescence (Fig. 5). Furthermore, contractions persisted after treatment with ruthenium red, which also supports the conclusion that ruthenium red did not block Ca^{2+} release or reuptake by the sarcoplasmic reticulum to a biologically significant extent. Taken together, these findings indicate that the site of action of ruthenium red at the concentration used in our study is the mitochondrion and, most likely, the mitochondrial electrogenic Ca^{2+} uniporter.

In isolated mitochondria, the K_m and V_{max} of the ruthenium red-sensitive Ca^{2+} uniporter have long been considered inadequate to produce significant changes in intramitochondrial Ca^{2+} during the time course of a single contractile cycle at extramitochondrial free Ca^{2+} concentrations that occur in situ (Nicholls and Crompton, 1980; Gunter and Pfeiffer, 1990), an expectation confirmed in isolated, perifused mitochondria (Leisey et al., 1993). However, because rapid ruthenium red-sensitive mitochondrial

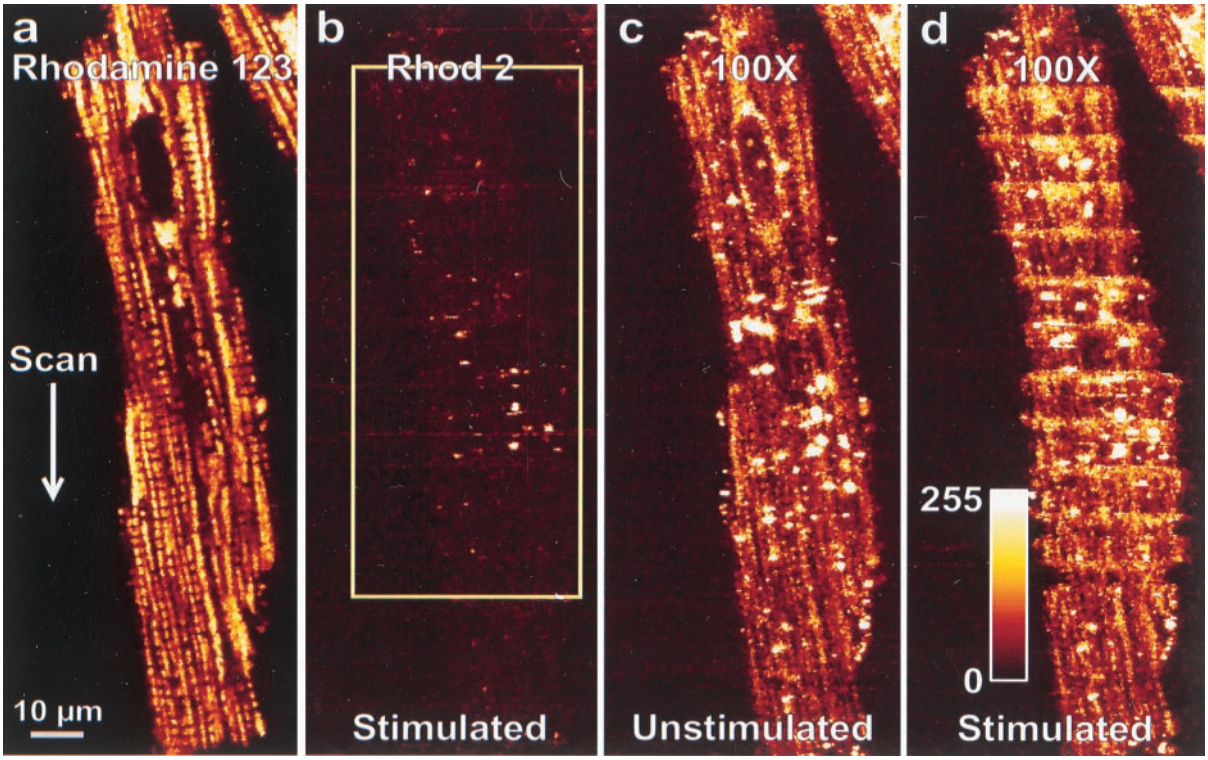

FIGURE 7 Discrimination by confocal microscopy of lysosomal and mitochondrial loading of Ca^{2+}-indicating fluorophores. A myocyte was loaded with Rhod 2-AM (5 μM) by the cold loading/warm incubation protocol and then with Rhodamine 123 (1 μM) for 30 min at 37°C. (*a*) Green Rhodamine 123 fluorescence documents the distribution of mitochondria within a myocyte. (*b*) A red fluorescence image of Rhod 2 was then collected during electrical stimulation at 1 Hz. Laser excitation was attenuated in *b*, so that none of the pixels were saturated (gray level less than 255). The Rhod 2 image so obtained showed heterogeneous punctate fluorescence that did not correspond to the Rhodamine 123-labeled mitochondria in *a*. Moreover, no fluorescence banding occurred as a consequence of electrical stimulation. (*c*) The myocyte was imaged again at 100 times more excitation energy, but without electrical stimulation. At a 100-fold greater excitation energy, fluorescence arising from lysosomes was now saturated, and a mitochondrial pattern of fluorescence emerged as a background to the original lysosomal pattern. (*d*) An identical image was collected, except during electrical stimulation at 1 Hz. In this last image, the background mitochondrial fluorescence showed horizontal banding that indicated Ca^{2+} transients.

Ca^{2+} uptake actually occurred in single living myocytes during the contractile cycle, our results indicate that the K_m of the uniporter is decreased and/or the V_{max} is increased in vivo for Ca^{2+} uptake by mitochondria. The presence in vivo of factors stimulating mitochondrial Ca^{2+} uptake, such as polyamines (Nicchitta and Williamson, 1984), may explain the difference between in vitro and in vivo observations.

In intact myocytes, adrenergic stimulation also increases the rate of mitochondrial Ca^{2+} uptake. In previous work, we measured cytosolic and mitochondrial Ca^{2+} transients in

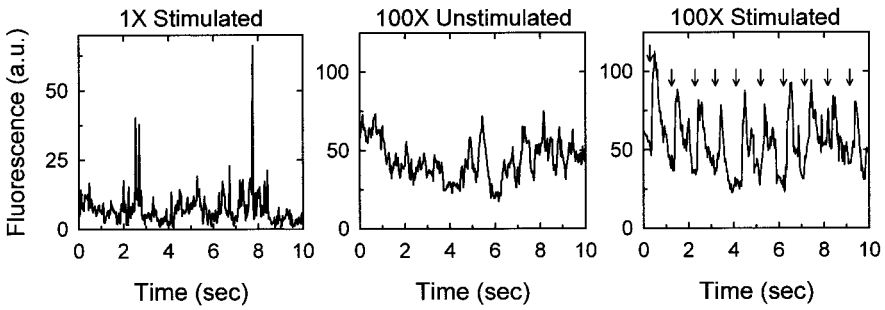

FIGURE 8 Plot analysis of Rhod 2 fluorescence transients at low and high excitation energy. Plot analyses were performed on the selected area outlined in yellow in Fig. 7. In each plot, the average pixel intensity in arbitrary units (a.u.) for each row of pixels in the *x* direction was plotted against the scan time calculated from *y* axis position. The left, middle, and right panels were taken from Fig. 7 *b* (1× excitation energy with stimulation), Fig. 7 *c* (100× excitation energy without stimulation), and Fig. 7 *d* (100× excitation energy with stimulation), respectively. Note the absence of regular transients in the left and middle panels, whereas repeating transients at 1 Hz are evident in the right panel (*arrows*).

both the presence and absence of the β-adrenergic agonist isoproterenol (Chacon et al., 1996; Ohata et al., 1998). Isoproterenol increases the rate of rise, the rate of recovery, and the amplitude of mitochondrial Ca^{2+} transients. Because hearts at high rates of work are generally under adrenergic stimulation and several earlier studies by others used adrenergic stimulation, we always used isoproterenol in the experiments reported in the present study.

Mechanisms of rapid mitochondrial Ca^{2+} uptake during the contractile cycle

A recently described rapid mode for mitochondrial Ca^{2+} uptake may also contribute to the mitochondrial Ca^{2+} transients observed during the contractile cycle (Sparagna et al., 1995; Gunter et al., 1998). In response to micromolar pulses of Ca^{2+}, the rapid uptake mode catalyzes an initial rate of mitochondrial Ca^{2+} uptake that is two to six times greater than steady-state mitochondrial uptake, but which quickly resets to the slower rate. Ruthenium red inhibits and spermine, ATP, and GTP activate the rapid mode of Ca^{2+} uptake. In situ, the repetitive turning on and off of the rapid mode of Ca^{2+} uptake in response to cytosolic Ca^{2+} transients may be responsible for generating and sharpening the mitochondrial Ca^{2+} transients.

Ca^{2+} released from the endoplasmic reticulum may also be preferentially accumulated by mitochondria because of the close anatomical relationship between the two organelles, as suggested for mitochondrial Ca^{2+} uptake after IP_3-induced Ca^{2+} mobilization in HeLa cells expressing aequorin in mitochondria (Rizzuto et al., 1993, 1998). Mitochondria and endoplasmic reticulum are closely adjacent in cells (Rizzuto et al., 1998; Mannella et al., 1998). In cardiac myocytes, Ca^{2+} released from the sarcoplasmic reticulum may be disproportionately accumulated by mitochondria because of relatively increased local Ca^{2+} concentrations in the vicinity of mitochondria. Similarly, preferential Ca^{2+} uptake may be promoted by the physical proximity of mitochondria to the sarcolemma (Gallitelli et al., 1999) or the t-tubules. Our data, however, indicate that the hypothesized preferential pathway from Ca^{2+}-releasing organelles, such as the sarcoplasmic reticulum, sarcolemma, and t-tubule, to the mitochondrial matrix space still involves the ruthenium red-sensitive mitochondrial Ca^{2+} uniporter.

Impact of lysosomal loading of Ca^{2+}-indicating fluorophores on measurements of mitochondrial Ca^{2+} transients by confocal microscopy versus microfluorometry

Although lysosomes were small in size and number compared to mitochondria, they accounted for the majority of noncytosolic fluorescence from myocytes after ester loading. Prominent lysosomal localization occurred after both warm and cold ester loading, even under the conditions of warm loading that prevented mitochondrial dye uptake (compare Figs. 3 *a* and 5 *a′* with Figs. 1 *a*, 5 *a*, 6, and 7 *b*; see also Chacon et al., 1994, 1996; Trollinger et al., 1997; Ohata et al., 1998). Consequently, when cytosolic fluorescence was selectively depleted after ester loading of Ca^{2+}-indicating fluorophores by warm incubation, total cellular fluorescence reported a predominantly lysosomal/endosomal signal. Ratiometric determinations under such circumstances do not eliminate the lysosomal contribution to the total fluorometric signal. These findings underscore the necessity for imaging techniques that distinguish mitochondria from other organelles in the study of mitochondrial Ca^{2+} fluxes in intact myocytes during the contractile cycle.

Previously we suggested that species differences might explain differences between observations by confocal microscopy that show mitochondrial Ca^{2+} transients in rabbit myocytes (Chacon et al., 1996; Trollinger et al., 1997; Ohata et al., 1998) and observations from microfluorometry that do not show these transients in myocytes from some other species, such as rat (Miyata et al., 1991; Di Lisa et al., 1993; Griffiths et al., 1997). Here we show, however, that rabbit myocytes do not differ from the rat myocytes of previous studies, because transients of total cellular fluorescence of Ca^{2+}-indicating fluorophores loaded into the noncytosolic compartment were not observed in rabbit myocytes (Figs. 7 and 8). In contrast, confocal imaging of individual mitochondria did reveal transients in rabbit myocytes. Thus differing methodologies applied to the same myocyte in the same experiment led to apparently different outcomes. Lysosomal loading accounted for the discrepancy, because the majority of noncytosolic fluorescence after ester loading of Ca^{2+}-indicating fluorophores into rabbit myocytes arose from the lysosomal/endosomal compartment. Mitochondria loaded to a much smaller extent. Only confocal imaging could distinguish the relatively weak mitochondrial fluorescence from the bright lysosomal fluorescence.

In general, lysosomal accumulation of ester-loaded fluorophores will depend on many factors, including loading temperature, ester concentration, the particular fluorophore used, the culture conditions, and the cell type and species of origin. One recent study utilizing microfluorometry describes transients during electrical pacing of the noncytosolic fluorescence of the Ca^{2+} indicator Indo-1 in guinea pig cardiac myocytes but not in rat myocytes (Griffiths, 1999). However, in this and earlier studies utilizing microfluorometry, the contribution of lysosomes to noncytosolic fluorescence was not assessed. When total noncytosolic fluorescence was measured in the present study, rabbit cardiac myocytes behaved identically to the rat cardiac myocytes of earlier work. Only by confocal imaging could the obscuring effect of lysosomal loading be circumvented and mitochondrial Ca^{2+} transients revealed. If myocytes from rat and rabbit are indeed different in their mitochondrial Ca^{2+} handling, then they must also be opposite in their lysosomal

uptake of ester-loaded Ca^{2+} indicators. Future studies will be needed to better assess these possible species differences.

Mitochondrial Ca^{2+} and myocardial metabolism

Myocardium exquisitely matches its ATP production to its ATP demand (Achterberg, 1988; Taegtmeyer, 1988). Mitochondrial free Ca^{2+} may be one factor that helps match mitochondrial energy production to myocardial energy demand (McCormack and Denton, 1979; Williamson and Cooper, 1980; Hansford, 1981; Moreno-Sanchez, 1985a,b; Halestrap, 1987). Our work presented here demonstrates that changes in mitochondrial free Ca^{2+} mediated by uptake through the ruthenium red-sensitive mitochondrial uniporter are kinetically competent to contribute to the close temporal matching of energy supply to energy demand in heart tissue. However, future experiments will be needed to determine whether suppression of mitochondrial Ca^{2+} transients compromises the mitochondrial ATP supply required for contractile function. In conclusion, our findings add to the increasing body of evidence in a variety of cell types that mitochondrial free Ca^{2+} responds rapidly to physiological signals potentially to exert control over mitochondrial metabolism (Wendt-Gallitelli and Isenberg, 1991; Rizzuto et al., 1992, 1993, 1998; Isenberg et al., 1993; Hajnoczky et al., 1995; Chacon et al., 1996; Jou et al., 1996; Trollinger et al., 1997; Bowser et al., 1998; Ohata et al., 1998; Robb-Gaspers et al., 1998; Gallitelli et al., 1999).

This work was supported, in part, by grant N00014-96-0283 from the Office of Naval Research and Program Project grant 5-P01 HL27430 from the National Institutes of Health. DRT is a recipient of a Research Training Fellowship in Experimental Cardiology through grant 5-T32 HL07793 from the National Institutes of Health. We also acknowledge core imaging facility support through National Institutes of Health grants 1-P50-AA11605 and 5-P30-DK34987.

REFERENCES

Achterberg, P. W. 1988. Adenine nucleotides, purine metabolism and myocardial function. *In* Myocardial Energy Metabolism. J. W. De Jong, editor. Kluwer Academic, Boston. 45–52.

Bowser, D. N., T. Minamikawa, P. Nagley, and D. A. Williams. 1998. Role of mitochondria in calcium regulation of spontaneously contracting cardiac muscle cells. *Biophys. J.* 75:2004–2014.

Calviello, G., and M. Chiesi. 1989. Rapid kinetic analysis of the calcium release channels of skeletal sarcoplasmic reticulum: the effect of inhibitors. *Biochemistry.* 28:1301–1306.

Chacon, E., H. Ohata, I. S. Harper, D. R. Trollinger, B. Herman, and J. J. Lemasters. 1996. Mitochondrial free calcium transients during excitation-contraction in rabbit cardiac myocytes. *FEBS Lett.* 382:31–36.

Chacon, E., J. M. Reece, A.-L. Nieminen, G. Zahrebelski, B. Herman, and J. J. Lemasters. 1994. Distribution of electrical potential, pH, free Ca^{2+}, and cell volume inside cultured adult rabbit cardiac myocytes during chemical hypoxia: a multiparameter digitized confocal microscopic study. *Biophys. J.* 66:942–952.

Chamberlain, B. K., P. Volpe, and S. Fleischer. 1984. Inhibition of calcium-induced calcium release from purified cardiac sarcoplasmic reticulum vesicles. *J. Biol. Chem.* 259:7547–7553.

Chiesi, M., R. Schwaller, and G. Calviello. 1988. Inhibition of rapid Ca-release from isolated skeletal and cardiac sarcoplasmic reticulum (SR) membranes. *Biochem. Biophys. Res. Commun.* 154:1–8.

Di Lisa, F., G. Gambassi, H. Spurgeon, and R. G. Hansford. 1993. Intramitochondrial free calcium in cardiac myocytes in relation to dehydrogenase activation. *Cardiovasc. Res.* 27:1840–1844.

Gallitelli, M. F., M. Schultz, G. Isenberg, and F. Rudolf. 1999. Twitch-potentiation increases calcium in peripheral more than in central mitochondria of guinea-pig ventricular myocytes. *J. Physiol. (Lond.).* 518(Part 2):433–447.

Golovina, V. A., and M. P. Blaustein. 1997. Spatially and functionally distinct Ca^{2+} stores in sarcoplasmic and endoplasmic reticulum. *Science.* 275:1643–1648.

Griffiths, E. J. 1999. Species dependence of mitochondrial calcium transients during excitation-contraction coupling in isolated cardiomyocytes. *Biochem. Biophys. Res. Commun.* 263:554–559.

Griffiths, E. J., C. J. Ocampo, J. S. Savage, G. A. Rutter, R. G. Hansford, M. D. Stern, and H. S. Silverman. 1998. Mitochondrial calcium transporting pathways during hypoxia and reoxygenation in single rat cardiomyocytes. *Cardiovasc. Res.* 39:423–433.

Griffiths, E. J., M. D. Stern, and H. S. Silverman. 1997. Measurement of mitochondrial calcium in single living cardiomyocytes by selective removal of cytosolic indo 1. *Am J. Physiol.* 273:C37–C44.

Gunter, T. E., L. Buntinas, G. C. Sparagna, and K. K. Gunter. 1998. The Ca^{2+} transport mechanisms of mitochondria and Ca^{2+} uptake from physiological-type Ca^{2+} transients. *Biochim. Biophys. Acta.* 1366:5–15.

Gunter, T. E., and D. R. Pfeiffer. 1990. Mechanisms by which mitochondria transport calcium. *Am. J. Physiol.* 258:C755–C768.

Hajnoczky, G., L. D. Robb-Gaspers, M. B. Seitz, and A. P. Thomas. 1995. Decoding of cytosolic calcium oscillations in the mitochondria. *Cell.* 82:415–425.

Halestrap, A. P. 1987. The regulation of the oxidation of fatty acids and other substrates in rat heart mitochondrial by changes in the matrix volume induced by osmotic strength, valinomycin and Ca^{2+}. *Biochem. J.* 244:159–164.

Hansford, R. G. 1981. Effect of micromolar concentrations of free Ca^{2+} ions on pyruvate dehydrogenase interconversion in intact rat heart mitochondria. *Biochem. J.* 194:721–732.

Isenberg, G., S. Han, A. Schemer, and M. F. Wendt-Gallitelli. 1993. Changes in mitochondrial calcium concentration during the cardiac contraction cycle. *Cardiovasc. Res.* 27:1800–1809.

Jou, M. J., T. I. Peng, and S-S. Sheu. 1996. Histamine induces oscillations of mitochondrial free Ca^{2+} concentration in single cultured rat brain astrocytes. *J. Physiol. (Lond).* 497:299–308.

Leisey, J. R., L. W. Grotyohann, D. A. Scott, and R. C. Scaduto, Jr. 1993. Regulation of cardiac mitochondrial calcium by average extramitochondrial calcium. *Am. J. Physiol.* 265:H1203–H1208.

Mannella, C. A., K. Buttle, B. K. Rath, and M. Marko. 1998. Electron microscopic tomography of rat-liver mitochondria and their interaction with the endoplasmic reticulum. *Biofactors.* 8:225–228.

Matlib, M. A., Z. Zhou, S. Knight, S. Ahmed, K. M. Choi, J. Krause-Bauer, R. Phillips, R. Altschuld, Y. Katsube, N. Sperelakis, and D. M. Bers. 1998. Oxygen-bridged dinuclear ruthenium amine complex specifically inhibits Ca^{2+} uptake into mitochondria in vitro and in situ in single cardiac myocytes. *J. Biol. Chem.* 273:10223–10231.

McCormack, J. G., and R. M. Denton. 1979. The effects of calcium ions and adenine nucleotides on the activity of pig heart 2-oxoglutarate dehydrogenase complex. *Biochem. J.* 180:533–544.

Miyata, H., E. G. Lakatta, M. D. Stern, and H. S. Silverman. 1992. Relation of mitochondrial and cytosolic free calcium to cardiac myocyte recovery after exposure to anoxia. *Circ. Res.* 71:605–613.

Miyata, H., H. S. Silverman, S. J. Sollott, E. G. Lakatta, M. D. Stern, and R. G. Hansford. 1991. Measurement of mitochondrial free Ca^{2+} contraction in living single rat cardiac myocytes. *Am. J. Physiol.* 261: H1123–H1134.

Moore, C. L. 1971. Specific inhibition of mitochondrial Ca^{2+} transport by ruthenium red. *Biochem. Biophys. Res. Commun.* 42:298–305.

Moravec, C. S., and M. Bond. 1991. Calcium is released from the junctional sarcoplasmic reticulum during cardiac muscle contraction. *Am. J. Physiol.* 260:H989–H987.

Moreno-Sanchez, R. 1985a. Contribution of the translocator of adenine nucleotides and the ATP synthase to the control of oxidative phosphorylation and arsenylation in liver mitochondria. *J. Biol. Chem.* 260: 4028–4034.

Moreno-Sanchez, R. 1985b. Regulation of oxidative phosphorylation in mitochondria by external free Ca^{2+} concentrations. *J. Biol. Chem.* 260:12554–12560.

Nicchitta, C. V., and J. R. Williamson. 1984. Spermine. A regulator of mitochondrial calcium cycling. *J. Biol. Chem.* 259:12978–12983.

Nicholls, D. G., and M. Crompton. 1980. Mitochondrial calcium transport. *FEBS Lett.* 111:261–268.

Nieminen, A.-L., T. L. Dawson, G. J. Gores, T. Kawanishi, B. Herman, and J. J. Lemasters. 1990. Protection by acidotic pH and fructose against lethal injury to rat hepatocytes from mitochondrial inhibition, ionophores and oxidant chemicals. *Biochem. Biophys. Res. Commun.* 167: 600–606.

Nieminen, A.-L., A. K. Saylor, B. Herman, and J. J. Lemasters. 1994. ATP depletion rather than mitochondrial depolarization mediates hepatocyte killing after metabolic inhibition. *Am. J. Physiol.* 267:C67–C74.

Nieminen, A-L., A. K. Saylor, S. A. Tesfai, B. Herman, and J. J. Lemasters. 1995. Contribution of the mitochondrial permeability transition to lethal injury after exposure of hepatocytes to *t*-butylhydroperoxide. *Biochem. J.* 307:99–106.

Ohata, H., E. Chacon, S. A. Tesfai, I. S. Harper, B. Herman, and J. J. Lemasters. 1998. Mitochondrial Ca^{2+} transients in cardiac myocytes during the excitation-contraction cycle: effects of pacing and hormonal stimulation. *J. Bioenerg. Biomembr.* 30:207–222.

Reed, K. C., and F. L. Bygrave. 1974. The inhibition of mitochondrial calcium transport by lanthanides and ruthenium red. *Biochem. J.* 140: 143–155.

Rizzuto, R., M. Brini, M. Murgia, and T. Pozzan. 1993. Microdomains with high Ca^{2+} close to IP_3-sensitive channels that are sensed by neighboring mitochondria. *Science.* 262:744–747.

Rizzuto, R., P. Pinton, W. Carrington, F. S. Fay, K. E. Fogarty, L. M. Lifshitz, R. A. Tuft, and T. Pozzan. 1998. Close contacts with the endoplasmic reticulum as determinants of mitochondrial Ca^{2+} responses. *Science.* 280:1763–1766.

Rizzuto, R., A. W. M. Simpson, M. Brini, and T. Pozzan. 1992. Rapid changes of mitochondrial Ca^{2+} revealed by specifically targeted recombinant aequorin. *Nature.* 358:325–332.

Robb-Gaspers, L. D., P. Burnett, G. A. Rutter, R. M. Denton, R. Rizzuto, and A. P. Thomas. 1998. Integrating cytosolic calcium signals into mitochondrial metabolic responses. *EMBO J.* 17:4987–5000.

Sparagna, G. C., K. K. Gunter, S. S. Sheu, and T. E. Gunter. 1995. Mitochondrial calcium uptake from physiological-type pulses of calcium. A description of the rapid uptake mode. *J. Biol. Chem.* 270: 27510–27515.

Taegtmeyer, H. 1988. Principles of fuel metabolism in heart muscle. *In* Myocardial Energy Metabolism. J.W. De Jong, editor. Kluwer Academic, Boston. 17–34.

Trollinger, D. R., W. E. Cascio, and J. J. Lemasters. 1997. Selective loading of Rhod 2 into mitochondria shows mitochondrial Ca^{2+} transients during the contractile cycle in adult rabbit cardiac myocytes. efficient between LysoTracker. *Biochem. Biophys. Res. Commun.* 236: 738–742.

Wendt-Gallitelli, M. F., and G. J. Isenberg. 1991. Total and free myoplasmic calcium during a contraction cycle: x-ray microanalysis in guinea-pig ventricular myocytes. *J. Physiol. (Lond.).* 435:349–372.

Williamson, J. R., and. R. H. Cooper. 1980. Regulation of the citric acid cycle in mammalian systems. *FEBS Lett.* 117(Suppl.):K73–K85.